

# First Evidence of a Retrograde Orbit of Transiting Exoplanet HAT-P-7b\*

Norio NARITA,<sup>1</sup> Bun'ei SATO,<sup>2</sup> Teruyuki HIRANO,<sup>3</sup> Motohide TAMURA<sup>1</sup>

<sup>1</sup> *National Astronomical Observatory of Japan, 2-21-1 Osawa, Mitaka, Tokyo, 181-8588, Japan  
norio.narita@nao.ac.jp*

<sup>2</sup> *Global Edge Institute, Tokyo Institute of Technology, 2-12-1 Ookayama, Meguro, Tokyo, 152-8550,  
Japan*

<sup>3</sup> *Department of Physics, The University of Tokyo, Tokyo, 113-0033, Japan*

(Received 2008 August 5; accepted 2008 August 27)

## Abstract

We present the first evidence of a retrograde orbit of the transiting exoplanet HAT-P-7b. The discovery is based on a measurement of the Rossiter-McLaughlin effect with the Subaru HDS during a transit of HAT-P-7b, which occurred on UT 2008 May 30. Our best-fit model shows that the spin-orbit alignment angle of this planet is  $\lambda = -132.6^\circ \pm_{-16.3}^{+10.5}$ . The existence of such a retrograde planet have been predicted by recent planetary migration models considering planet-planet scattering processes or the Kozai migration. Our finding provides an important milestone that supports such dynamic migration theories.

**Key words:** stars: planetary systems: individual (HAT-P-7) — stars: rotation — techniques: radial velocities — techniques: spectroscopic

## 1. Introduction

One of the surprising properties of extrasolar planets is their distributions around their host stars. Since many Jovian planets have been found in the vicinity (far inside the snow line) of their host stars, numbers of theoretical models have been studied to explain inward planetary migration. Recently understanding of planetary migration mechanisms has rapidly progressed through observations of the Rossiter-McLaughlin effect (hereafter the RM effect: Rossiter 1924, McLaughlin 1924) in transiting exoplanetary systems. The RM effect is an apparent radial velocity anomaly during planetary transits. By measuring this effect, one can learn the sky-projected angle between the stellar spin axis and the planetary orbital axis,

---

\* Based on data collected at Subaru Telescope, which is operated by the National Astronomical Observatory of Japan.

denoted by  $\lambda$  (see Ohta et al. 2005; Gaudi & Winn 2007 for theoretical discussion).

So far, spin-orbit alignment angles of about 15 transiting planets have been measured (Fabrycky & Winn 2009, and references therein). Among those RM targets, significant spin-orbit misalignments have been reported for 3 transiting planets: XO-3b (Hébrard et al. 2008; Winn et al. 2009a), HD80606b (Moutou et al. 2009; Pont et al. 2009; Winn et al. 2009b), and WASP-14b (Johnson et al. 2009). These misaligned planets are considered to have migrated through planet-planet scattering processes (e.g., Rasio & Ford 1996; Marzari & Weidenschilling 2002; Nagasawa et al. 2008; Chatterjee et al. 2008) or Kozai cycles with tidal evolution (e.g., Wu & Murray 2003; Takeda & Rasio 2005; Fabrycky & Tremaine 2007; Wu et al. 2007), rather than the standard Type II migration (e.g., Lin & Papaloizou 1985; Lin et al. 1996; Ida & Lin 2004).

The existence of such misaligned planets has demonstrated validity of the planetary migration models considering planet-planet scattering or the Kozai migration. On the other hand, such planetary migration models also predict significant populations of “retrograde” planets. Thus discoveries of retrograde planets would be an important milestone for confirming the predictions of recent planetary migration models, and intrinsically interesting.

In this letter, we report the first evidence of such a retrograde planet in the transiting exoplanetary system HAT-P-7. Section 2 summarizes the target and our Subaru observations, and section 3 describes the analysis procedures for the RM effect. Section 4 presents results and discussion for the derived system parameters. Finally, section 5 summarizes the main findings of this letter.

## 2. Target and Subaru Observations

HAT-P-7 is an F6 star at a distance of 320 pc hosting a very hot Jupiter (Pál et al. 2008; hereafter P08). Among transiting-planet host stars, F type stars are interesting RM targets because these stars often have a large stellar rotational velocity, which facilitates measurements of the RM effect. However, the rotational velocity of HAT-P-7 is  $V \sin I_s = 3.8 \text{ km s}^{-1}$  (P08), which is unusually slower than expected for an F6 type star. Nevertheless, this system is favorable for the RM observations, since the star is relatively bright ( $V = 10.5$ ) and the expected amplitude of the RM effect ( $V \sin I_s (R_p/R_s)^2 \sim 20 \text{ m s}^{-1}$ ) is sufficiently detectable with the Subaru telescope.

We observed a full transit of HAT-P-7b with the High Dispersion Spectrograph (HDS: Noguchi et al. 2002) on the Subaru 8.2m telescope on UT 2008 May 30. We employed the standard I2a set-up of the HDS, covering the wavelength range  $4940 \text{ \AA} < \lambda < 6180 \text{ \AA}$  and used the Iodine gas absorption cell for radial velocity measurements. The slit width of  $0''.6$  yielded a spectral resolution of  $\sim 60000$ . The seeing on that night was around  $0''.6$ . The exposure time for radial velocity measurements was 6-8 minutes, yielding a typical signal-to-noise ratio (SNR)

of approximately 120 per pixel. We processed the observed frames with standard IRAF<sup>1</sup> procedures and extracted one-dimensional spectra. We computed relative radial velocities following the algorithm of Butler et al. (1996) and Sato et al. (2002), as described in Narita et al. (2007). We estimated the internal error of each radial velocity as the scatter in the radial-velocity solutions among  $\sim 4$  Å segments of the spectrum. The typical internal error was  $\sim 5$  m s<sup>-1</sup>. The radial velocities and uncertainties are summarized in table 1.

### 3. Analyses

We model the RM effect of HAT-P-7 following the procedure of Winn et al. (2005), as described in Narita et al. (2009) and Hirano et al. in prep. We start with a synthetic template spectrum, which matches for the stellar property of HAT-P-7 described in P08, using a synthetic model by Coelho et al. (2005). To model the disk-integrated spectrum of HAT-P-7, we apply a rotational broadening kernel of  $V \sin I_s = 3.8$  km s<sup>-1</sup> and assume limb-darkening parameters for the spectroscopic band as  $u_1 = 0.45$  and  $u_2 = 0.31$ , based on a model by Claret (2004). We then subtract a scaled copy of the original unbroadened spectrum with a velocity shift to simulate spectra during a transit. We create numbers of such simulated spectra using different values of the scaling factor  $f$  and the velocity shift  $v_p$ , and compute the apparent radial velocity of each spectrum. We thereby determine an empirical formula that describes the radial velocity anomaly  $\Delta v$  in HAT-P-7 due to the RM effect, and find

$$\Delta v = -fv_p \left[ 1.444 - 0.623 \left( \frac{v_p}{V \sin I_s} \right)^2 \right]. \quad (1)$$

For radial velocity fitting, including the Keplerian motion and the RM effect, we adopt stellar and planetary parameters based on P08 as follows; the stellar mass  $M_s = 1.47 [M_\odot]$ , the stellar radius  $R_s = 1.84 [R_\odot]$ , the radius ratio  $R_p/R_s = 0.0763$ , the orbital inclination  $i = 85.7^\circ$ , and the semi-major axis in units of the stellar radius  $a/R_s = 4.35$ . We assess possible systematic errors due to uncertainties in the fixed parameters in section 4. We also include a stellar jitter of 3.8 m s<sup>-1</sup> for the P08 Keck data as systematic errors of radial velocities by quadrature sum. It enforces the ratio of  $\chi^2$  contribution and the degree of freedom for the Keck data to be unity. We do not include additional radial velocity errors for the Subaru data, because we find the ratio for the Subaru dataset is already smaller than unity (as described in section 4).

In addition, we adopt the transit ephemeris  $T_c = 2453790.2593$  [HJD] and the orbital period  $P = 2.2047299$  days based on P08. Note that this ephemeris has an uncertainty of 3 minutes for the observed transit; however the uncertainty is well within our time-resolution (exposure time of 6-8 minutes and readout time of 1 minute) and is negligible for our purpose. The adopted parameters above are summarized in table 2.

---

<sup>1</sup> The Image Reduction and Analysis Facility (IRAF) is distributed by the U.S. National Optical Astronomy Observatories, which are operated by the Association of Universities for Research in Astronomy, Inc., under cooperative agreement with the National Science Foundation.

Our model has 3 free parameters describing the HAT-P-7 system: the radial velocity semi-amplitude  $K$ , the sky-projected stellar rotational velocity  $V \sin I_s$ , and the sky-projected angle between the stellar spin axis and the planetary orbital axis  $\lambda$ . We fix the eccentricity  $e$  to zero, and the argument of periastron  $\omega$  is not considered. Finally we add two offset velocity parameters for respective radial velocity datasets ( $v_1$ : our Subaru dataset,  $v_2$ : the Keck dataset in P08).

We then calculate the  $\chi^2$  statistic (hereafter “main-case”)

$$\chi^2 = \sum_i \left[ \frac{v_{i,\text{obs}} - v_{i,\text{calc}}}{\sigma_i} \right]^2, \quad (2)$$

where  $v_{i,\text{obs}}$  and  $\sigma_i$  are observed radial velocities and uncertainties, and  $v_{i,\text{calc}}$  are radial velocity values calculated based on a Keplerian motion and on the empirical RM formula given above.

We determine optimal orbital parameters by minimizing the  $\chi^2$  statistic using the AMOEBA algorithm (Press et al. 1992). We estimate  $1\sigma$  uncertainty of each free parameter based on the criterion  $\Delta\chi^2 = 1.0$  when a parameter is stepped away from the best-fit value and the other parameters are re-optimized.

We also fit the radial velocities using another statistic function for reference (hereafter “test-case”),

$$\chi^2 = \sum_i \left[ \frac{v_{i,\text{obs}} - v_{i,\text{calc}}}{\sigma_i} \right]^2 + \left[ \frac{V \sin I_s - 3.8}{0.5} \right]^2. \quad (3)$$

The last term is *a priori* constraint for  $V \sin I_s$  to match the independent spectroscopic analysis by P08.

#### 4. Results and Discussion

Figure 1 shows observed radial velocities and the best-fit model curve for the main-case. Figure 2 illustrates the RM effect of HAT-P-7b with the best-fit model and also shows a comparison with the case of  $\lambda = 0^\circ$  and  $V \sin I_s = 3.8 \text{ km s}^{-1}$  model. The upper panel of figure 3 plots a  $\chi^2$  contour in  $(\lambda, V \sin I_s)$  space. As a result, we find the key parameter  $\lambda = -132.6^\circ (+10.5^\circ, -16.3^\circ)$ , implying a retrograde orbit of HAT-P-7b. The stellar rotational velocity is  $V \sin I_s = 2.3 (+0.6, -0.5) \text{ km s}^{-1}$ , which is marginally consistent with the P08 spectroscopic result ( $V \sin I_s = 3.8 \pm 0.5 \text{ km s}^{-1}$ ). Residuals from the best-fit model indicate rms of  $4.14 \text{ m s}^{-1}$  for the Subaru dataset and  $4.09 \text{ m s}^{-1}$  for the P08 Keck dataset. The rms of the Subaru residuals is well within our internal radial velocity errors, and that of the Keck residuals is in good agreement with the assumed jitter level of  $3.8 \text{ m s}^{-1}$ . One may wonder that a smaller  $V \sin I_s$  allowed in the main-case would weaken the detection-significance of the RM effect. However, since  $V \sin I_s = 0 \text{ km s}^{-1}$  is excluded by  $\Delta\chi^2 = 36.49$ , there is very little chance that a true  $V \sin I_s$  is actually nearly zero and a spin-orbit alignment angle  $\lambda$  is very small. The lower panel of figure 3 plots a similar  $\chi^2$  contour but for the test-case. In this case,

we find  $\lambda = -122.5^\circ (+6.4^\circ, -7.7^\circ)$  and  $V \sin I_s = 3.1 \pm 0.4 \text{ km s}^{-1}$ . Thus our two results (main and test cases) are well consistent with each other. In addition, we test the fitting with the eccentricity  $e$  and the argument of periastron  $\omega$  as free parameters. As a result, we do not find any significant (nonzero) eccentricity for this planet. The best-fit parameters and uncertainties are summarized in table 3.

In the above analyses, we fixed several parameters as summarized in table 2, which were based on P08 and Claret (2004). In order to estimate the level of possible systematic errors, we retry the fitting for following four cases; (1)  $a/R_s = 4.63$ ,  $i = 89.2^\circ$  (corresponding to  $1\sigma$  lower limit of the impact parameter in P08); (2)  $a/R_s = 3.97$ ,  $i = 82.6^\circ$  (corresponding to  $1\sigma$  upper limit of the impact parameter in P08); (3)  $u_1 = 0.65$  (a greater limb-darkening case); and (4)  $u_1 = 0.25$  (a smaller limb-darkening case).

Consequently, we find that respective results for  $\lambda$  and  $V \sin I_s$  are; (1)  $\lambda = -151.8^\circ (+11.1^\circ, -12.8^\circ)$  and  $V \sin I_s = 2.1 \pm 0.4 \text{ km s}^{-1}$ ; (2)  $\lambda = -99.5^\circ (+3.0^\circ, -6.2^\circ)$  and  $V \sin I_s = 7.6 \pm 2.9 \text{ km s}^{-1}$ ; (3)  $\lambda = -135.9^\circ (+11.2^\circ, -16.7^\circ)$  and  $V \sin I_s = 2.2 \pm 0.5 \text{ km s}^{-1}$ ; and (4)  $\lambda = -129.8^\circ (+9.9^\circ, -15.6^\circ)$  and  $V \sin I_s = 2.4 \pm 0.6 \text{ km s}^{-1}$ . Thus  $\lambda = -164.6^\circ - -96.5^\circ$  and  $V \sin I_s = 1.7 - 10.5 \text{ km s}^{-1}$  can be still probable if the uncertainties for fixed parameters (especially for the impact parameter) are taken into account. These systematic errors would be significantly reduced when the Kepler photometric data for HAT-P-7 are available (Borucki et al. 2009).

The derived value of  $\lambda$  seems to indicate a retrograde orbit by itself. However, since the true spin-orbit angle  $|\Psi|$  also depends on the inclination of the stellar spin axis  $I_s$ ,  $|\Psi|$  is not necessarily greater than  $90^\circ$  (corresponding to a retrograde orbit) even if  $\lambda = -132.6^\circ$ . Thus one might wonder whether the planet HAT-P-7b is statistically in a retrograde orbit. We can roughly estimate the probability using the relation of spherical geometry,

$$\cos |\Psi| = \cos I_s \cos i + \sin I_s \sin i \cos \lambda. \quad (4)$$

Note that  $I_s$  ranges from  $0^\circ$  to  $180^\circ$ . We compute the true spin-orbit angle  $|\Psi|$  of HAT-P-7b by substituting the observed values of  $i$  and  $\lambda$  into the relation. We adopt  $i = 85.7^\circ$  (P08) and test three representative cases for  $\lambda$  ( $-164.6^\circ$ ,  $-132.6^\circ$ , and  $-96.5^\circ$ ). Assuming an uniform distribution for  $\cos I_s$  within the range of value, the probabilities of a retrograde orbit ( $|\Psi| > 90^\circ$ ) are 99.85% ( $\lambda = -164.6^\circ$ ), 99.70% ( $\lambda = -132.6^\circ$ ), and 91.65% ( $\lambda = -96.5^\circ$ ), respectively. We note that  $|\Psi|$  is always larger than  $85.7^\circ$  (the adopted value of  $i$ , in the case of  $I_s = 0^\circ$ ). Those estimates favor a retrograde orbit of HAT-P-7b.

On the other hand, it is important to point out that the stellar rotational velocity  $V \sin I_s = 3.8 \text{ km s}^{-1}$  determined by the spectroscopic analysis (P08) is exceptionally slow for an F6 star. For example, HAT-P-2 and TrES-4, which are other known planetary host stars with similar spectral type, have larger stellar rotational velocities:  $V \sin I_s = 19.8 \text{ km s}^{-1}$  (HAT-P-2, Bakos et al. 2007 and also confirmed from the RM effect by Winn et al. 2007) and

$V \sin I_s = 8.5 \text{ km s}^{-1}$  (TrES-4, Sozzetti et al. 2009 and also confirmed from the RM effect by Narita et al. in prep.). The small  $V \sin I_s$  may suggest a smaller inclination angle of the stellar spin axis. In that case, it is highly possible that the planet is in a nearly polar retrograde orbit.

We note that too small  $I_s$  can be constrained by the facts that a faster stellar rotation of HAT-P-7 than  $500 \text{ km s}^{-1}$  would be physically unlikely due to stellar break-up, and that a faster rotation than  $100 \text{ km s}^{-1}$  would be empirically unlikely for a F6 star (Gray 2005). Translating the constraints into  $\cos I_s$ , we find a probability of such unrealistic cases is only  $\sim 0.03\%$ , which has very little impact on the probability estimations for a retrograde orbit. In any case, it would be important to directly constrain  $I_s$  by other observational methods (e.g., Henry & Winn 2008 or asteroseismology with the Kepler) in order to estimate a true spin-orbit angle of HAT-P-7b.

We previously experienced a false positive of a spin-orbit misalignment in HD17156b due to lower precision radial velocity data (Narita et al. 2008; Narita et al. 2009). The problem for the HD17156 case (Narita et al. 2008) was that radial velocity uncertainties were comparable with predicted RM amplitude and also due to a poor number of radial velocity samples. Based on the lesson, we estimate the significance of our RM detection using the equation (26) in Gaudi & Winn (2007). As a result, the SNR of our RM detection is over 10, and thus we conclude to have obtained radial velocities of a sufficient number and precision to model the RM effect of HAT-P-7b.

Nevertheless, we finally note that we should care about possible systematic errors in  $\lambda$ . Since the RM amplitude of HAT-P-7b is only  $\sim 15 \text{ m s}^{-1}$ , any systematic shift as much as several  $\text{m s}^{-1}$  due to stellar jitter or other reasons at ingress or egress phase would cause a large systematic difference in  $\lambda$ . Thus further radial velocity measurements for this interesting system are desired to confirm a retrograde orbit of HAT-P-7b more decisively.

## 5. Summary

We observed a full transit of HAT-P-7b with the Subaru 8.2m telescope on UT 2008 May 30, and measured the RM effect of this planet. Based on the RM modeling, we discovered the first evidence of a retrograde orbit of HAT-P-7b. This is the first discovery of a retrograde extrasolar planet. The existence of such planets have been indeed predicted in some recent planetary migration models considering planet-planet scattering and/or the Kozai migration (e.g., Fabrycky & Tremaine 2007; Wu et al. 2007; Nagasawa et al. 2008; Chatterjee et al. 2008). In addition, it is interesting to point out that HAT-P-7b is the first spin-orbit misaligned planet having no significant eccentricity. This discovery may suggest that other hot Jupiters in circular orbits also have significant spin-orbit misalignments or even retrograde orbits. Thus further RM observations for transiting planets, including not only eccentric or binary system planets but also close-in circular planets, would be encouraged in order to understand populations of aligned/misaligned/retrograde planets.

*Note added after submission* — Winn et al. (2009c) report an independent evidence for a retrograde orbit of HAT-P-7b, based on independent Subaru HDS observations conducted in 2009 June/July.

We acknowledge the invaluable support for our Subaru observations by Akito Tajitsu, a support scientist for the Subaru HDS. We are grateful to Yasushi Suto, Ed Turner, Wako Aoki, and Toru Yamada for helpful discussions on this study; Josh Winn and his colleagues for sharing their information in advance of publication. This paper is based on data collected at Subaru Telescope, which is operated by the National Astronomical Observatory of Japan. The data analysis was in part carried out on common use data analysis computer system at the Astronomy Data Center, ADC, of the National Astronomical Observatory of Japan. N.N. is supported by a Japan Society for Promotion of Science (JSPS) Fellowship for Research (PD: 20-8141). We wish to acknowledge the very significant cultural role and reverence that the summit of Mauna Kea has always had within the indigenous Hawaiian community.

## References

- Bakos, G. Á., et al. 2007, *ApJ*, 670, 826  
Borucki, W. J., et al. 2009, *Science*, 325, 709  
Butler, R. P., Marcy, G. W., Williams, E., McCarthy, C., Dosanjuh, P., & Vogt, S. S. 1996, *PASP*, 108, 500  
Chatterjee, S., Ford, E. B., Matsumura, S., & Rasio, F. A. 2008, *ApJ*, 686, 580  
Claret, A. 2004, *A&A*, 428, 1001  
Coelho, P., Barbuy, B., Meléndez, J., Schiavon, R. P., & Castilho, B. V. 2005, *A&A*, 443, 735  
Fabrycky, D., & Tremaine, S. 2007, *ApJ*, 669, 1298  
Fabrycky, D. C., & Winn, J. N. 2009, *ApJ*, 696, 1230  
Gaudi, B. S., & Winn, J. N. 2007, *ApJ*, 655, 550  
Gray, D. F. 2005, *The Observation and Analysis of Stellar Photospheres*  
Hébrard, G., et al. 2008, *A&A*, 488, 763  
Henry, G. W., & Winn, J. N. 2008, *AJ*, 135, 68  
Ida, S., & Lin, D. N. C. 2004, *ApJ*, 616, 567  
Johnson, J. A., Winn, J. N., Albrecht, S., Howard, A. W., Marcy, G. W., & Gazak, J. Z. 2009, arXiv:0907.5204  
Lin, D. N. C., Bodenheimer, P., & Richardson, D. C. 1996, *Nature*, 380, 606  
Lin, D. N. C., & Papaloizou, J. 1985, in *Protostars and Planets II*, ed. D. C. Black & M. S. Matthews, 981–1072  
Marzari, F., & Weidenschilling, S. J. 2002, *Icarus*, 156, 570  
McLaughlin, D. B. 1924, *ApJ*, 60, 22  
Moutou, C., et al. 2009, *A&A*, 498, L5  
Nagasawa, M., Ida, S., & Bessho, T. 2008, *ApJ*, 678, 498

- Narita, N., Sato, B., Ohshima, O., & Winn, J. N. 2008, PASJ, 60, L1+
- Narita, N., et al. 2007, PASJ, 59, 763
- Narita, N., et al. 2009, arXiv:0905.4727
- Noguchi, K., et al. 2002, PASJ, 54, 855
- Ohta, Y., Taruya, A., & Suto, Y. 2005, ApJ, 622, 1118
- Pál, A., et al. 2008, ApJ, 680, 1450 (P08)
- Pont, F., et al. 2009, A&A, 502, 695
- Press, W. H., Teukolsky, S. A., Vetterling, W. T., & Flannery, B. P. 1992, Numerical recipes in C. The art of scientific computing (Cambridge: University Press, —c1992, 2nd ed.)
- Rasio, F. A., & Ford, E. B. 1996, Science, 274, 954
- Rossiter, R. A. 1924, ApJ, 60, 15
- Sato, B., Kambe, E., Takeda, Y., Izumiura, H., & Ando, H. 2002, PASJ, 54, 873
- Sozzetti, A., et al. 2009, ApJ, 691, 1145
- Takeda, G., & Rasio, F. A. 2005, ApJ, 627, 1001
- Winn, J. N., et al. 2005, ApJ, 631, 1215
- Winn, J. N., et al. 2007, ApJL, 665, L167
- Winn, J. N., et al. 2009a, ApJ, 700, 302
- Winn, J. N., et al. 2009b, arXiv:0907.5205
- Winn, J. N., Johnson, J. A., Albrecht, S., Howard, A. W., Marcy, G. W., Crossfield, I. J., & Holman, M. J. 2009c, arXiv:0908.1672
- Wu, Y., & Murray, N. 2003, ApJ, 589, 605
- Wu, Y., Murray, N. W., & Ramsahai, J. M. 2007, ApJ, 670, 820



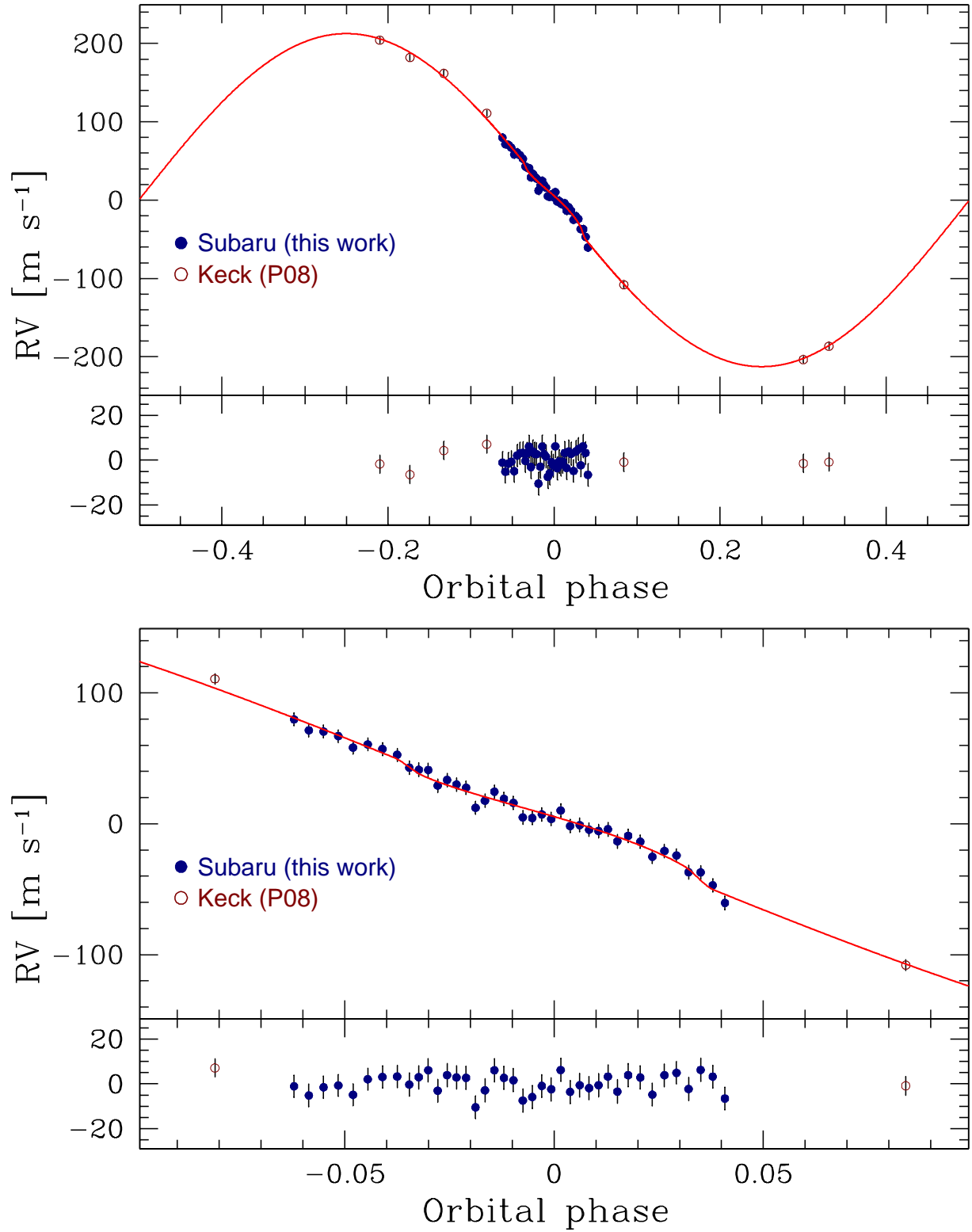


**Fig. 1.** Upper panels: Radial velocities and the best-fit curve of HAT-P-7 as a function of orbital phase. The upper figure show the entire orbit and the lower figure do the zoom of transit phase. Bottom panels: Residuals from the best-fit curve.

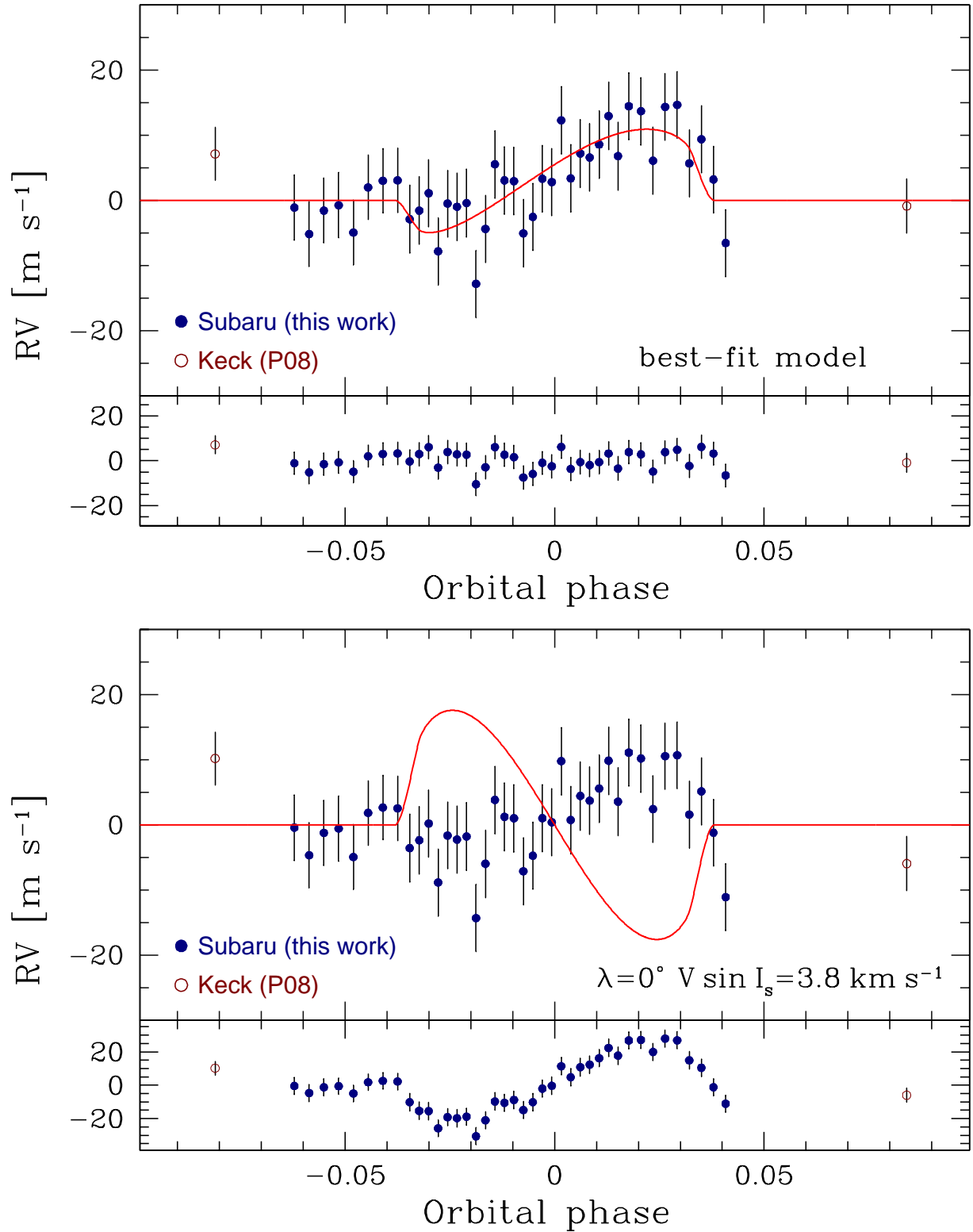


**Fig. 2.** Upper figure: The RM effect of HAT-P-7b. The upper panel shows difference radial velocities (namely, the Keplerian motion is subtracted from the original radial velocities). The solid line indicates the best-fit RM model. The lower panel plots residuals from the best-fit model. Lower figure: The case for  $\lambda = 0^\circ$  and  $V \sin I_s = 3.8 \text{ km s}^{-1}$  model, for reference.

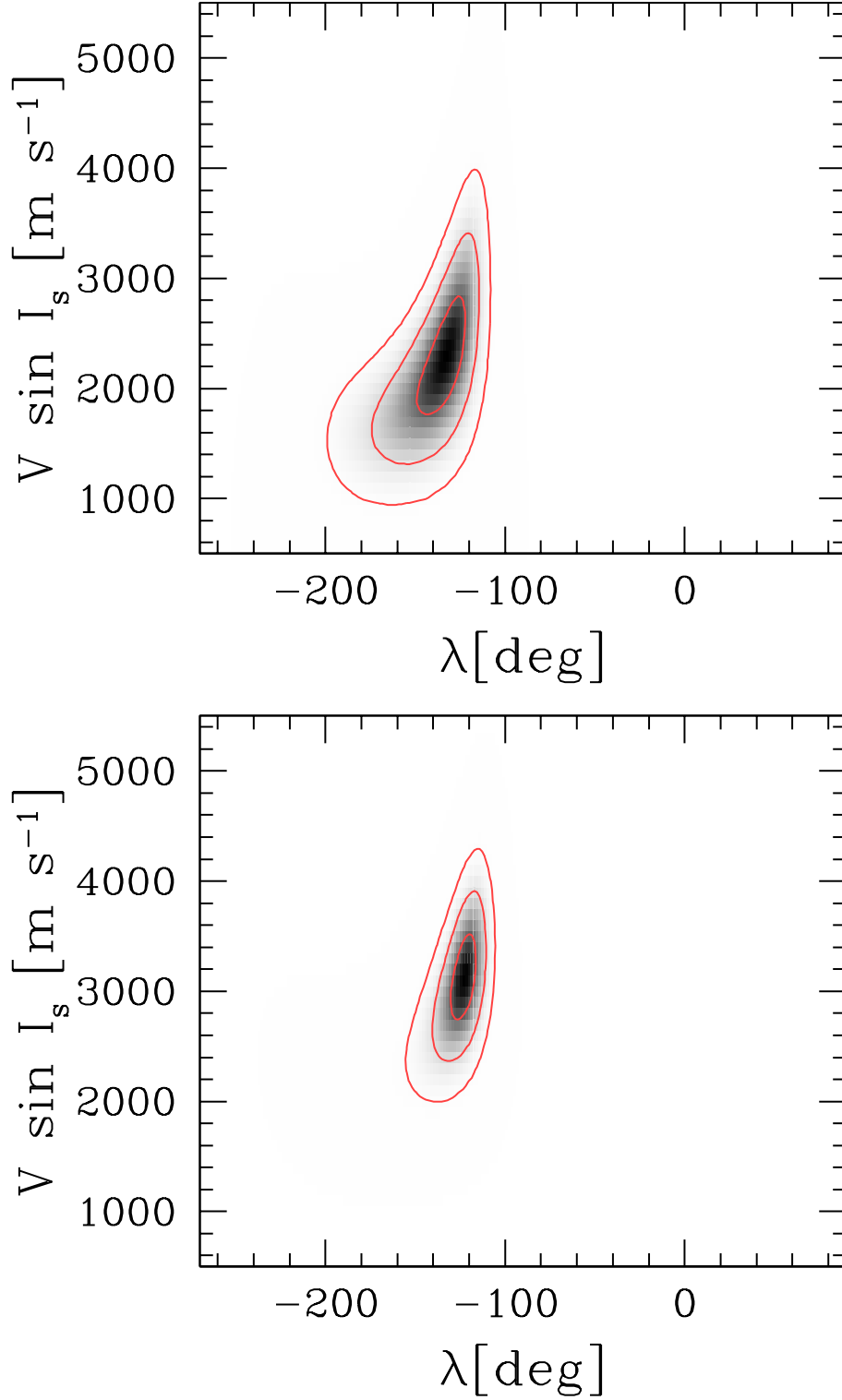


**Fig. 3.** Plots of  $(\lambda, V \sin I_s)$  contours of HAT-P-7 based on our Subaru dataset and the P08 Keck dataset without (upper) and with (lower) the *a priori* constraint on  $V \sin I_s$ . The solid lines show  $\Delta\chi^2 = 1.0, 4.0,$  and  $9.0$  (from inner to outer), respectively.

**Table 1.** Radial velocities obtained with the Subaru/HDS.

Time [HJD]	Value [m s <sup>-1</sup> ]	Error [m s <sup>-1</sup> ]
2454616.89606	65.07	5.02
2454616.90384	56.63	5.00
2454616.91160	55.84	4.98
2454616.91936	52.22	5.03
2454616.92712	43.55	5.00
2454616.93489	45.98	4.98
2454616.94264	42.45	4.94
2454616.95039	37.97	4.94
2454616.95678	28.22	5.20
2454616.96176	26.60	5.17
2454616.96674	26.32	5.15
2454616.97172	14.40	5.17
2454616.97670	18.77	5.11
2454616.98167	15.30	5.15
2454616.98666	12.88	5.21
2454616.99165	-2.53	5.18
2454616.99663	2.91	5.16
2454617.00161	9.84	5.17
2454617.00661	4.34	5.19
2454617.01159	1.23	5.17
2454617.01657	-9.81	5.16
2454617.02156	-10.32	5.16
2454617.02655	-7.47	5.13
2454617.03154	-11.00	5.15
2454617.03652	-4.53	5.17
2454617.04151	-16.47	5.16
2454617.04650	-15.68	5.23
2454617.05147	-19.28	5.16
2454617.05645	-20.31	5.21
2454617.06142	-18.94	5.17
2454617.06640	-28.10	5.21
2454617.07206	-23.85	5.16
2454617.07842	-28.44	5.18
2454617.08479	-39.88	5.13
2454617.09115	-35.41	5.09

**Table 1.** (Continued.)

2454617.09751	-38.90	5.13
2454617.10389	-51.68	5.15
2454617.11026	-51.74	5.16
2454617.11664	-61.71	5.12
2454617.12301	-75.20	5.14

**Table 2.** Adopted stellar and planetary parameters.

Parameter	Value	Source
$M_s [M_\odot]$	1.47	P08
$R_s [R_\odot]$	1.84	P08
$R_p/R_s$	0.0763	P08
$i [^\circ]$	85.7	P08
$a/R_s$	4.35	P08
$u_1$	0.45	Claret (2004)
$u_2$	0.31	Claret (2004)
$T_c$ [HJD]	2453790.2593	P08
$P$ [days]	2.2047299	P08

**Table 3.** Best-fit values and uncertainties of the free parameters.

Parameter	main-case		test-case	
	Value	Uncertainty	Value	Uncertainty
$K$ [m s <sup>-1</sup> ]	212.6	±1.9	213.3	±1.9
$V \sin I_s$ [km s <sup>-1</sup> ] <sup>a</sup>	2.3	<sup>+0.6</sup> <sub>-0.5</sub>	3.1	±0.4
$\lambda$ [°] <sup>a</sup>	-132.6	<sup>+10.5</sup> <sub>-16.3</sub>	-122.5	<sup>+6.4</sup> <sub>-7.7</sub>
$v_1$ [m s <sup>-1</sup> ]	-14.7	±1.6	-16.6	±1.3
rms (Subaru) [m s <sup>-1</sup> ]	4.14		4.32	
$v_2$ [m s <sup>-1</sup> ]	-37.4	±1.6	-37.5	±1.6
rms (Keck) [m s <sup>-1</sup> ]	4.09		4.09	

<sup>a</sup>: Systematic errors are not included in the uncertainties (see text).